ARTICLE

Excess of De Novo Deleterious Mutations in Genes Associated with Glutamatergic Systems in Nonsyndromic Intellectual Disability

Fadi F. Hamdan,[1] Julie Gauthier,[2] Yoichi Araki,[3] Da-Ting Lin,[3] Yuhki Yoshizawa,[4] Kyohei Higashi,[4] A-Reum Park,[5] Dan Spiegelman,[2] Sylvia Dobrzeniecka,[2] Amélie Piton,[2] Hideyuki Tomitori,[4] Hussein Daoud,[2] Christine Massicotte,[1] Edouard Henrion,[2] Ousmane Diallo,[2] S2D Group,[2] Masoud Shekarabi,[2] Claude Marineau,[2] Michael Shevell,[6] Bruno Maranda,[7] Grant Mitchell,[1] Amélie Nadeau,[1] Guy D'Anjou,[1] Michel Vanasse,[1] Myriam Srour,[1] Ronald G. Lafrenière,[2] Pierre Drapeau,[8] Jean Claude Lacaille,[9] Eunjoon Kim,[10] Jae-Ran Lee,[5] Kazuei Igarashi,[4] Richard L. Huganir,[3] Guy A. Rouleau,[2] and Jacques L. Michaud[1,*]

Little is known about the genetics of nonsyndromic intellectual disability (NSID). We hypothesized that de novo mutations (DNMs) in synaptic genes explain an important fraction of sporadic NSID cases. In order to investigate this possibility, we sequenced 197 genes encoding glutamate receptors and a large subset of their known interacting proteins in 95 sporadic cases of NSID. We found 11 DNMs, including ten potentially deleterious mutations (three nonsense, two splicing, one frameshift, four missense) and one neutral mutation (silent) in eight different genes. Calculation of point-substitution DNM rates per functional and neutral site showed significant excess of functional DNMs compared to neutral ones. De novo truncating and/or splicing mutations in *SYNGAP1*, *STXBP1*, and *SHANK3* were found in six patients and are likely to be pathogenic. De novo missense mutations were found in *KIF1A*, *GRIN1, CACNG2*, and *EPB41L1*. Functional studies showed that all these missense mutations affect protein function in cell culture systems, suggesting that they may be pathogenic. Sequencing these four genes in 50 additional sporadic cases of NSID identified a second DNM in *GRIN1* (c.1679_1681dup/p.Ser560dup). This mutation also affects protein function, consistent with structural predictions. None of these mutations or any other DNMs were identified in these genes in 285 healthy controls. This study highlights the importance of the glutamate receptor complexes in NSID and further supports the role of DNMs in this disorder.

Introduction

Intellectual disability (ID) is defined by significant limitations in adaptive behavior and intellectual function that occur before 18 years of age. ID affects up to 3% of the general population and can be broadly divided into a syndromic form associated with morphologic and/or metabolic abnormalities and a nonsyndromic form characterized by the absence of these distinguishing features. The majority of the genes identified so far in nonsyndromic ID (NSID) are either X-linked or autosomal recessive.[1,2] Although an autosomal-dominant mode of inheritance is not frequently observed in NSID because of the reduced reproductive fitness associated with this condition, autosomal-dominant mutations arising de novo may explain a large fraction of cases.

A growing body of work suggests that disruption of glutamatergic synapses plays an important role in common neurodevelopmental disorders, such as ID, autism spectrum disorders (MIM 209850), and schizophrenia (MIM 181500).[1,3,4] The majority of excitatory synapses in the central nervous system use L-glutamate as a neurotransmitter. Glutamate receptors can be classified into those that form ion channel pores upon binding glutamate (AMPA receptors [AMPARs], NMDA receptors [NMDARs], kainate receptors [KARs]) and those that indirectly activate ion channels through a signaling cascade that involves G proteins (metabotropic glutamate receptors [mGluRs]). Proteomic studies showed that NMDARs and mGluRs are components of large protein complexes (NMDAR complex of ~185 proteins; mGluR5 complex of ~52 proteins), whereas AMPARs interact with a smaller number of proteins, with all three groups totaling at least 221 proteins.[5] These synaptic glutamate receptor complexes (referred to herein as GRCs) are enriched in proteins involved in synaptic plasticity and learning and memory,[6–9] thus constituting attractive candidate genes for neurocognitive diseases such as ID. The importance of the glutamatergic pathways in such conditions is highlighted by the fact that pathogenic mutations in genes encoding four glutamate receptors, *GRIA3* (MIM 305915), *GRIK2* (MIM 138244), *GRIN2A* (MIM

[1]Centre of Excellence in Neuromics of Université de Montréal, Sainte-Justine Hospital Research Centre, Montréal H3T1C5, Canada; [2]Centre of Excellence in Neuromics of Université de Montréal, Centre Hospitalier de l'Université de Montréal Research Centre and the Department of Medicine, Montréal H2L2W5, Canada; [3]Department of Neuroscience and Howard Hughes Medical Institute, Johns Hopkins University School of Medicine, Baltimore, MD 21205, USA; [4]Graduate School of Pharmaceutical Sciences, Chiba University, Chiba 260-8675, Japan; [5]Korea Research Institute of Bioscience and Biotechnology, Daejeon 305-806, Korea; [6]Department of Neurology and Neurosurgery, Montréal's Children's Hospital, McGill University, Montréal H3H1P3, Canada; [7]Department of Pediatrics, Centre Hospitalier Universitaire Laval, Québec G1V4G2, Canada; [8]Department of Pathology and Cell Biology and Le Groupe de Recherche sur le Système Nerveux Central, Université de Montréal, Montréal H3C3J7, Canada; [9]Le Groupe de Recherche sur le Système Nerveux Central, Department of Physiology, Université de Montréal, Montréal H3C3J7, Canada; [10]Department of Biological Sciences, Korea Advanced Institute of Science and Technology, Daejeon 305-701, Korea
*Correspondence: jacques.michaud@recherche-ste-justine.qc.ca
DOI 10.1016/j.ajhg.2011.02.001.

138253), and *GRIN2B* (MIM 138252), have been identified in ID.[1,10–12]

We hypothesized that de novo mutations (DNMs) in genes encoding members of the GRC could explain an important fraction of the sporadic NSID cases. To explore this, we sequenced 197 genes encoding glutamate receptors and a large subset of their known interacting proteins in sporadic cases of NSID. We found DNMs in 11% of the patients. Genetic and functional observations indicate that the majority of the identified mutations affect protein function and may be pathogenic.

Subjects and Methods

Subjects and Sample Collection

The initial cohort of sporadic NSID cases (n = 95; 46 males, 49 females), most of whom were French Canadian, is described elsewhere.[13] In the context of this study, NSID was defined with the following criteria: (1) diagnosis of ID established on a clinical basis via standardized developmental or IQ tests, (2) absence of specific dysmorphic features, as assessed by an experienced clinical geneticist, (3) birth weight and postnatal growth within normal limits, (4) normal head circumference at birth, (5) absence of risk factors such as neonatal asphyxia, prematurity, or exposure to teratogenic drugs, (6) negative results for the following standard investigations: cytogenetic studies (karyotyping, subtelomeric fluorescence in situ hybridization, or comparative genomic hybridization studies) and molecular testing for the common expansion mutation in *FMR1* (MIM 309550), and (7) absence of dysgenetic or specific changes on brain CT scan or MRI. The second cohort of sporadic NSID cases (n = 50; 27 males, 23 females), also mainly of French Canadian ethnicity, was recruited according to the same patient selection criteria. A population control group of 285 healthy French Canadians was also collected. Blood samples were obtained from all members of these series and from each of their parents after obtaining written informed consent and approval from institutional ethics committees. Paternity and maternity of each individual of all families were confirmed by using six highly informative unlinked microsatellite markers (see Table S1 available online for marker primer sets).

Gene Selection

We focused our attention on a list of 221 nonredundant proteins, curated by the Genes to Cognition group, that were identified by proteomic studies of the NR1/NR2 (NMDAR complex: 185 proteins), mGluR5 (52 proteins), and GluR2 (8 proteins).[5] From these, we selected 109 candidate genes for resequencing that (1) code for a glutamate receptor, (2) are expressed predominantly in the brain, (3) are required for synaptic plasticity or neurotransmission, (4) influence synapse structure (synapse density, dendritic spine, neurite extension), or (5) are required for learning or memory. We selected 88 additional genes by searching PubMed for other NMDAR, AMPAR, or mGluR5 interactors that met at least one of these criteria and included all other brain-expressed glutamate receptors, resulting in a total of 197 selected genes (Table S2).

Gene Screening and Bioinformatics

PCR primers targeting all coding exons and boundary intronic (at least 50–100 bp from each side) junctions of the 197 GRC genes were designed with Exon-Primer from the UCSC Genome Browser (Table S3). PCR was done in 384-well plates with 5 ng of genomic DNA, according to standard procedures. The PCR products were sequenced at the McGill University and Genome Quebec Innovation Centre (Montréal, Canada) on a 3730XL DNA Analyzer. In each case, unique variants (nonrecurrent in the NSID cohort and not in the Database of Single Nucleotide Polymorphism [dbSNP131]) were further tested by reamplifying the fragment from blood DNA and by resequencing the proband and both parents with reverse and forward primers. PolyPHRED (version 5.04), PolySCAN (version 3.0), and Mutation Surveyor (version 3.10, Soft Genetics) were used for mutation detection.

Estimation of Base Pairs Screened

The total number of sequenced bases was estimated for each gene based on genomic coordinates of each amplicons successfully sequenced; we excluded the primer sequences from these estimates because the first ~20 bases from a sequencing read are usually either undetectable or of low quality. Overlapping amplicons were merged to form a single genomic interval, and coding and noncoding sequences for each gene were annotated according to the refFlat table from the UCSC Genome Browser. Nonsynonymous and synonymous sites were estimated at 71.2% and 28.8% of the coding sites, respectively, whereas the number of CpG sites was estimated at 2.8% of coding and at 1% of intronic sites, as previously described.[14]

Expression Constructs

Mutations in *KIF1A* (MIM 601255), *GRIN1* (MIM 138249), *CACNG2* (MIM 602911), and *EPB4L1* (MIM 602879) were introduced by site-directed mutagenesis into their corresponding positions in the published rat cDNA expression constructs encoding KIF1A motor domain (MD, aa 1–365)-EGFP,[15] NR1A,[16] NR2B,[16] myc-tagged stargazin,[17] and 4.1N,[18,19] respectively. For 4.1N, the human Pro^{854} position corresponds to Pro^{852} in the rat, which was mutated to serine herein by site-directed mutagenesis; for the sake of simplicity, we refer to it in Figure 3 as 4.1N-P854S.

Expression in Oocytes and Voltage-Clamp Recording

Xenopus laevis oocytes were coinjected with rat NR2B and either wild-type NR1 or NR1-E662K or NR1-S560dup complementary RNAs, and macroscopic currents were measured as previously described.[16]

Cell Culture, Transfection, Coimmunoprecipitation, Immunoblotting, and Immunofluorescence

These standard techniques were done as previously described for KIF1A[20] and EPB41L/4.1N.[18,19]

Structure Prediction of the NR1 Subunit

To build three-dimensional (3D) protein structure models, we used SWISS-MODEL Workspace, a Web-based integrated service dedicated to protein structure homology modeling.[21,22] The AMPA-sensitive rat GluA2 receptor (Protein Data Bank ID: 3KG2) and the rat NR1A subunit were selected as the template and the target sequence.[23] The target sequence was submitted to both "Automated Mode" and "Alignment Mode." The structures were visualized with PyMOL viewer version 0.99.

Recording of Miniature Excitatory Postsynaptic Current

Whole-cell recordings were made from cortical cultures. Small fire-polished patch electrodes (7–9 MΩ) were used. The series resistance in these recordings varied between 30 and 35 MΩ, and data sets in which series resistance varied more than 10% during

the recording were rejected for further analysis. No electronic compensation for series resistance was employed. The patch electrode solution contained the following: 115 mM $CsMeSO_4$, 0.4 mM EGTA, 5 mM TEA-Cl, 2.8 mM NaCl, 20 mM HEPES, 3 mM Mg-ATP, 0.5 mM Na-GTP, 10 mM Na-Phosphocreatine (pH 7.2), and osmolarity between 290 and 292 $mosmol^{-1}$. The extracellular solution was of the following composition: 143 mM NaCl, 5 mM KCl, 10 mM HEPES, 10 mM glucose, 2 mM $CaCl_2$, 0.0005 mM TTX, 0.1 mM Picrotoxin (pH 7.4), and osmolarity between 302 and 305 $mosmol^{-1}$. During the basal recording of miniature excitatory postsynaptic current (mEPSC), cells were voltage clamped at −65 mV. Electrophysiological data were acquired via a multiclamp 700B amplifier (Axon Instruments), and signals were digitized at 10 kHz and low pass filtered at 2 kHz.

Results

Sequence Variants Identified in the NSID Patients

We sequenced the coding exons and their intronic boundaries of 197 GRC genes (193 autosomal, four X-linked) in 95 patients with sporadic NSID (see Subjects and Methods for gene selection and Table S2 for gene list). We chose sporadic cases to increase the likelihood of finding pathogenic DNMs. On average, 95% of all amplicons were successfully sequenced, representing ~91 Mb of coding and ~85 Mb of flanking intronic diploid sequence. In total, we identified 2300 variants (1153 coding and 1147 intronic) (Table 1; see Table S4 for list of all variants). Of these, 646 variants were found only once in the NSID cohort and were not previously reported in the dbSNP131, including 225 nonsynonymous (four nonsense and 221 missense), 199 synonymous, seven insertions/deletions (INDELs; two out-of-frame INDELs, five in-frame INDELs), and four variants affecting the consensus canonical splice sites. Because these unique variants are more likely to be de novo, we further studied them by determining whether they were transmitted from one of the parents. In this set of 646 variants, we identified 11 DNMs, including three nonsense, one 1 bp deletion frameshift, two splicing, four missense, and one synonymous variant, all found in different patients (Table 2). The other unique variants were found to be transmitted from healthy parents and, therefore, are unlikely to be disease causing on their own. Clinical profiles of the patients with DNMs are outlined in Table 3.

Table 1. Summary of Identified Variants

Variant Class	Nonrecurrent				Recurrent			
	Total	dbSNP	Unique	DNM	Total	dbSNP	Not in dbSNP	Total
Nonsense	4	0	4	3	0	0	0	4
Missense	285	64	221	4	167	132	35	452
Silent	309	110	199	1	373	350	23	682
In-frame INDELS	5	0	5	0	8	4	4	13
Frameshift INDELS	2	0	2	1	0	0	0	2
Splice	4	0	4	2	0	0	0	4
Intronic	321	110	211	0	822	708	114	1143

Data from sequencing 197 glutamate receptor complex genes in 95 NSID cases. Nonrecurrent variants are those seen only once in the NSID cohort. Unique variants are those that are nonrecurrent and also not found in dbSNP131. Splice denotes variants in the canonical consensus splice sites (GT/AG). Intronic variants presented herein do not include canonical splice variants.

De Novo Truncating and Splicing Mutations

We identified three truncating DNMs in *SYNGAP1* (MIM 603384; c.412A>T/p.Lys138X; c.1735C>T/p.Arg579X; c.2438delT/p.Leu813ArgfsX23), as well as one truncating (c.1162C>T/p.Arg388X) and one splicing (c.169+1G>A) DNM in *STXBP1* (MIM 602926; Table 2). We recently reported the identification of these DNMs in *SYNGAP1* and *STXBP1* in patients with moderate-to-severe ID, and we reported the absence of DNMs or deleterious mutations in these two genes in 190 controls.[13,24] Another DNM, affecting the splice acceptor site in intron 5 (c.601-1G>A) of *SHANK3* (MIM 606230), was found in a male with mild ID and severe language impairment (Table 3). RT-PCR showed that this mutation interferes with the splicing of exon 6, resulting in a frameshift at position 211 and a premature stop codon (Figure S1). No truncating or splicing mutations were identified in *SHANK3* in 475 control individuals that we previously sequenced and reported elsewhere.[25,26]

Missense and Silent DNMs

De novo missense mutations were identified in *KIF1A* (c.296C>T/p.Thr99Met), *GRIN1* (c.1984G>A/p.Glu662Lys), *EPB41L1* (c.2560C>T/p.Pro854Ser), and *CACNG2* (c.427G>C/p.Val143Leu) (Table 2). These mutations affect evolutionarily conserved amino acid residues (Figure S2) and are predicted to affect protein function by widely used prediction algorithms (SIFT,[27] PloyPhen,[28] or Panther[29]). In addition, a de novo synonymous mutation (c.735A>G/p.Thr245Thr) was identified in *DRD1* (MIM 126449), which encodes for the dopamine receptor D1. This variant is unlikely to have any functional consequence, because it does not change the amino acid sequence and is not predicted to affect mRNA splicing. Sequencing these four genes in 50 additional patients with sporadic NSID identified a de novo in-frame 3 bp duplication in *GRIN1* (c.1679_1682dup/p.Ser560dup) (Table 2 and Table S4). These four genes were subsequently sequenced in 285 controls, and neither of these DNMs, nor any de novo or evidently deleterious mutations (such as truncating or splicing mutations), were identified (Table S5).

Functional Impact of p.Thr99Met on KIF1A

The KIF1A p.Thr99Met DNM was identified in a female with moderate ID (Table 3). *KIF1A* encodes a kinesin motor protein that transports synaptic vesicle precursors from the cell body to the tips of axons. KIF1A is composed of an N-terminal motor domain, followed by regulatory and

Table 2. DNMs Identified in NSID Patients

DNM	Gene	Chromosome	RefSeq Number	Protein (aa)	Predicted DNM Effect
Truncating/Splicing					
c.412A>T; p.Lys138X	*SYNGAP1*	6	NM_006772.2	1343	truncating
c.1735C>T; p.Arg579X	*SYNGAP1*	6	NM_006772.2	1343	truncating
c.2438delT; p.Leu813ArgfsX23	*SYNGAP1*	6	NM_006772.2	1343	truncating
c.1162C>T; p.Arg388X	*STXBP1*	9	NM_003165.3	603	truncating
c.169+1G>A (splicing)	*STXBP1*	9	NM_003165.3	603	truncating (RT-PCR-fs)
c.601-1G>A (splicing)	*SHANK3*	22	NM_01080420.1	1747	truncating (RT-PCR-fs)
Missense					
c.296C>T; p.Thr99Met	*KIF1A*	2	NM_004321.4	1690	damaging (SIFT, PolyPhen, Panther)
c.427G>C; p.Val143Leu	*CACNG2*	22	NM_006078.3	323	damaging (SIFT, PolyPhen, Panther)
c.2560C>T; p.Pro854Ser	*EPB41L1*	20	NM_012156.2	881	damaging (SIFT, PolyPhen, Panther)
c.1984G>A; p.Glu662Lys	*GRIN1*	9	NM_007327.3	938	damaging (Panther)
In-Frame Duplication[1]					
c.1679_1681dup; p.Ser560dup	*GRIN1*	9	NM_007327.3	938	NA
Synonymous					
c.735A>G; p.Thr245Thr	*DRD1*	5	NM_000794.3	446	neutral

RT-PCR-fs denotes transcripts detected by RT-PCR and found, by sequencing, to result in frameshifts. Damaging denotes according to predictions by SIFT, PolyPhen, or Panther. NA denotes not applicable.
[1] Not identified in the primary screen (NSID, n = 95) but found in the targeted secondary screen of a second cohort of NSID patients (n = 50).

cargo-binding domains.[30,31] Thr^{99} lies in the highly conserved p loop consensus ATP-binding site of the KIF1A motor domain (GQ$\underline{T}^{99}$XXGKT/S) (Figure S2). To determine whether p.Thr99Met affects KIF1A movement along neurites, we transfected primary rat hippocampal neurons with different KIF1A MD-EGFP fusion constructs, including wild-type (KIF1A-MD) or mutant motor domains containing either p.Thr99Met (KIF1A-MD-T99M) or p.Thr312Met (KIF1A-MD-T312M) mutation, which was previously shown to affect the motor activity of KIF1A.[15] KIF1A-MD

Table 3. Clinical Phenotype of the Patients with Functional DNMs

Patient	Gene	DNM	Age	Sex	ID	Epilepsy	Neurological Examination	MRI	CT Scan
Patient 1	*SYNGAP1*	p.Lys138X	4 yr 5 mo	F	++/+++	GEN	normal	normal	ND
Patient 2	*SYNGAP1*	p.Arg579X	5 yr 10 mo	F	++/+++	GEN	normal	normal	ND
Patient 3	*SYNGAP1*	p.Leu813ArgfsX23	12 yr 10 mo	F	++/+++	–	normal	ND	normal
Patient 4	*STXBP1*	p.Arg388X	15 yr	F	+++	PC	hypotonia	normal	normal
Patient 5	*STXBP1*	c.169-1G>A	27 yr	F	+++	PC	hypotonia	ND	normal
Patient 6[1]	*SHANK3*	c.601-1G>A	15 yr	M	+	–	normal	ND	normal
Patient 7	*KIF1A*	p.Thr99Met	3 yr 5 mo	F	+++	–	axial hypotonia/peripheral spasticity	atrophy[2]	ND
Patient 8	*GRIN1*	p.Glu662Lys	10 yr	F	++	–	normal	ND	normal
Patient 9	*GRIN1*	p.Ser560dup	7 yr 6 mo	M	+++	PC	hypotonia	normal	ND
Patient 10	*EPB41L1*	p.Pro854Ser	6 yr	M	+++	–	hypotonia	normal	ND
Patient 11	*CACNG2*	p.Val143Leu	8 yr	M	++	–	normal	normal	ND

Detailed clinical profiles of the patients (1–5) with DNMs in *SYNGAP1* and *STXBP1* were described elsewhere.[13,24] ID scale: + denotes mild, ++ denotes moderate, +++ denotes severe. The following abbreviations are used: ND, not determined; GEN, generalized epilepsy; PC, partial complex epilepsy.
[1] Assessment with the Autism Diagnostic Observation Schedule-Generic at 15 years of age was not suggestive of autism.
[2] Mild atrophy of the vermian region of the cerebellum on the MRI (Figure S5).

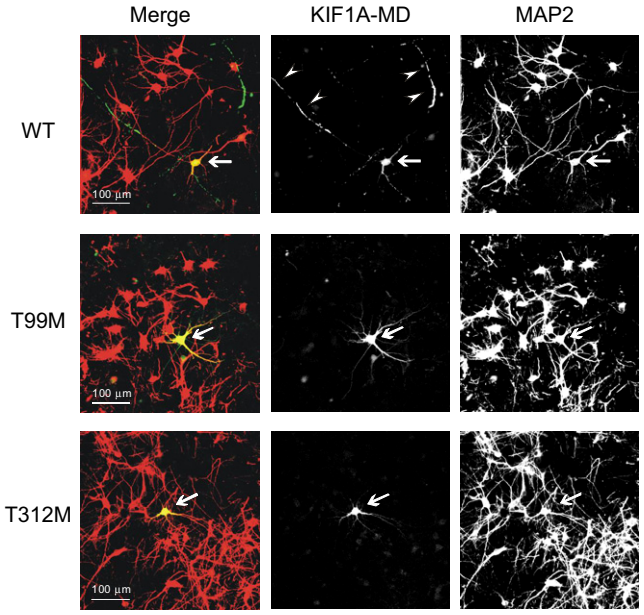

Figure 1. Impact of p.Thr99Met on KIF1A Subcellular Localization
EGFP-tagged motor domain (MD) constructs of KIF1A were expressed in cultured hippocampal neurons and visualized by immunofluorescence staining with an anti-EGFP. The MD of wild-type (WT) KIF1A (KIF1A-MD) accumulated in the axons (arrow heads), in contrast to KIF1A-MD-T99M or KIF1A-MD-T312M. The neuronal cell bodies and dendrites were stained with anti-MAP2 antibody.

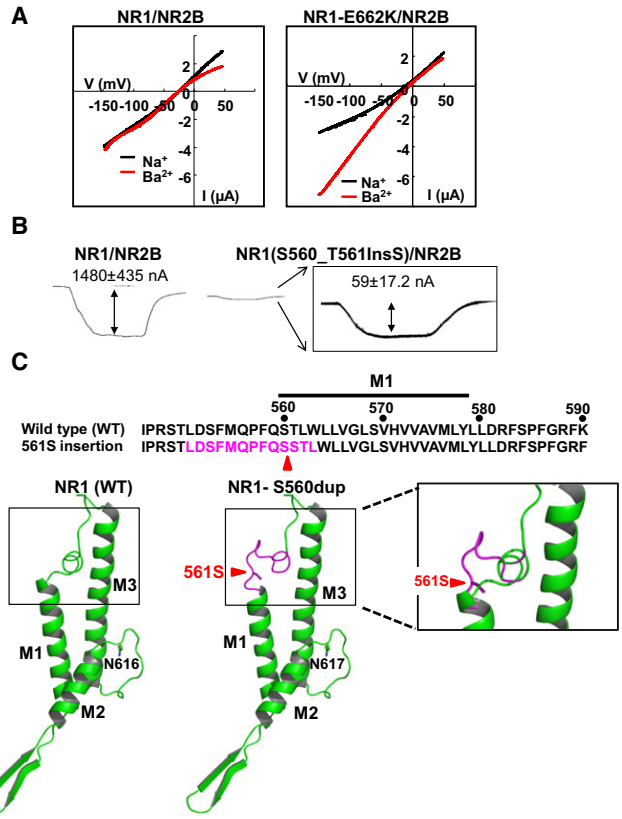

Figure 2. Impact of GRIN1 p.Glu662Lys and p.Ser560dup on NMDAR Function
Xenopus oocytes were coinjected with mRNAs of NR2B and either wild-type NR1 or mutated NR1 (E662K or S560dup).
(A) Current-voltage curves of Na^+ and Ba^{2+} currents. I-V curves for Glu+Gly-activated currents were measured by voltage ramps with Na saline and Ba saline.
(B) Inward current induced by 10 μM glycine and 10 μM glutamate (Vh = −70 mV) in oocytes coinjected with NR2B and either wild-type NR1 or NR1-S560dup mRNAs. Inset: enlargement of the mutant NR1 signal. Values are means ± standard error of the mean (SEM) of eight independent experiments.
(C) Conformational change of NR1 caused by p.Ser560dup. Top: amino acid sequences flanking the M1 transmembrane region are shown. The position of p.Ser560dup, resulting in the addition of a Ser561, is shown and indicated by an arrow head. Bottom: a 3D representation of the rat NR1 receptor subunit (WT and NR1-S560dup). M1, M2, and M3 represent transmembrane regions constituting the channel pore. The entrance to the channel pore (boxed) is significantly altered by the p.Ser560dup mutation.

accumulated in distal regions of neurites, whereas both KIF1A-MD-T312M and KIF1A-MD-T99M showed greatly reduced distal localization and increased accumulation throughout the cell body and proximal neurites (Figure 1).

Functional Impact of p.Glu662Lys and p.Ser560dup on GRIN1

The p.Glu662Lys mutation was identified in a female with mild-to-moderate ID, whereas the p.Ser560dup mutation was found in a male with severe ID and epilepsy (Table 3). *GRIN1* encodes the essential NMDAR subunit NR1, which associates with other subunits to form a heteromeric ligand-gated Ca^{2+} ion channel. The p.Glu662Lys DNM lies in the posttransmembrane (TM) region 3 of NR1, whereas p.Ser560dup is located just before TM1 (Figure S2). To test the effect of both mutations on NMDAR activity, we coinjected *Xenopus* oocytes with NR1/NR2B, NR1-E662K/NR2B, or NR1-S560dup/NR2B mRNAs and performed electrophysiology. To minimize Ca^{2+}-activated Cl^- currents, which could be toxic to the cells, we compared Ba^{2+} currents instead of Ca^{2+} currents with Na^+ currents in both NR1/NR2B and NR1-E662K/NR2B via voltage clamp. Ba^{2+} currents were greater than Na^+ currents in NR1-E662K/NR2B transfected cells, but both Ba^{2+} and Na^+ currents were nearly equal in NR1/NR2B transfected cells (Figure 2A). The affinity of the receptor to the agonist glycine and its response to Mg^{2+} block were not affected by p.Glu662Lys (Figure S3). Interestingly, the effect of p.Ser560dup was more pronounced, almost abolishing the activity of the receptor (Figure 2B). To test the effect of this insertion on the structure of the receptor, we built a three-dimensional model of the rat NR1A by using the available X-ray structure of the closely related rat GluA2 AMPAR[23] as a template and showed that the p.Ser560dup is predicted to significantly alter the 3D structure at the receptor's channel pore entrance (Figure 2C).

Impact of p.Pro854Ser on EPB41L1 Binding to AMPAR

The p.Pro854Ser in EPB41L1 was found in a male with severe ID (Table 3). *EPB41L1* encodes a neuronal cytoskeletal protein known as 4.1N, which binds to AMPAR subunits through its C-terminal domain and regulates

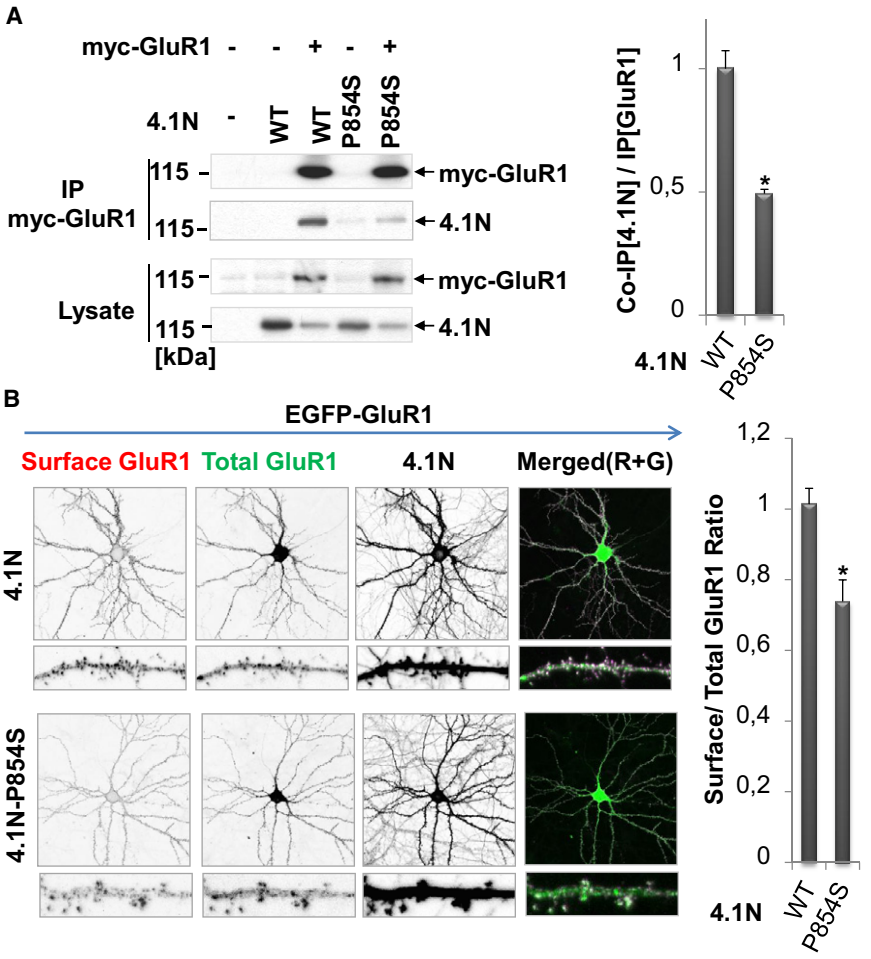

Figure 3. Functional Impact of the p.Pro854Ser EPB41L1 Mutation

(A) Indicated plasmid combinations (wild-type 4.1N [WT], 4.1N-P854S [P854S], myc-GluR) were cotransfected in HEK293 cells, and extracted proteins were immunoprecipitated with an anti-myc antibody and then analyzed by immunoblotting with anti-myc or anti-4.1N antibodies. The amount of coIP of 4.1N was reduced in the cells transfected with the 4.1N-P854S mutant. Right: the quantification of coIP experiment (mean ± SEM, n = 3, *p < 0.05, t test).

(B) Hippocampal neurons were cotransfected with GFP-GluR1 and the indicated 4.1N constructs. Surface GluR1 was stained by anti-GFP antibody in nonpermeabilized conditions and visualized by staining with a secondary anti-rabbit IgG (Alexa 568). Right: the quantification of GluR1 surface expression in presence of mutant or wild-type 4.1N (signal with WT adjusted to 1; mean ± SEM, n = 4, two-tailed Student's t test, *p < 0.05)

their expression at the synaptic membrane.[18,19] Because p.Pro854Ser affects a highly conserved residue in this C-terminal domain, we tested whether it disrupts the interaction of 4.1N with the AMPAR subunit GluR1 in transfected HEK293 cells. Coimmunoprecipitation (coIP) studies showed that p.Pro854Ser reduces the binding of 4.1N to GluR1 by 50% in these cells (Figure 3A). Moreover, insertion of the AMPAR subunit GluR1 at the synaptic membrane was significantly decreased in transfected hippocampal neurons producing mutant 4.1N when compared to cells producing wild-type 4.1N (Figure 3B).

Impact of p.Val143Leu on CACNG2 Binding to AMPAR

The DNM p.Val143Leu was identified in a male with moderate ID (Table 3). *CACNG2* encodes stargazin (also known as TARP-γ2), a synaptic adaptor protein that binds to AMPAR and regulates its synaptic trafficking, as well as its channel properties.[32,33] We investigated whether p.Val143Leu, which lies in the TM3 of stargazin, affects its interaction with AMPARs in transfected HEK293 cells. CoIP studies showed that p.Val143Leu significantly decreases stargazin's ability to bind to GluR1 or GluR2 AMPAR subunits in these cells (Figure 4A). In addition, cell surface expression of GluR1 was reduced in transfected hippocampal neurons (Figure 4B) and HEK293 cells (Figure S4) producing mutant stargazin, as compared to cells producing the wild-type protein. Consistent with these findings, expression of stargazin-V143L mutant decreased both miniEPSC amplitude and frequency in transfected hippocampal neurons, suggesting that p.Val143Leu caused a reduction in glutamatergic transmission (Figure 4C).

Excess of Functional De Novo Mutations in NSID

We next sought to determine whether the identified nonsynonymous or splicing (referred to herein as functional) point substitution DNMs (p.DNMs) were found in excess compared to neutral ones (nonsplicing intronic, synonymous) in our NSID cohort, which would suggest that a subset of these DNMs are pathogenic. We sequenced ~107 Mb (diploid) of neutral sites and identified only one synonymous p.DNM, resulting in a neutral p.DNM rate of 0.93×10^{-8} mutations per bp per generation. This result is consistent with direct DNM rate estimates ($\sim 1.0 \times 10^{-8}$) derived from recent family-based whole-genome sequencing control studies.[34,35] Based on our estimate of the neutral p.DNM rate, we would expect ~0.6 p.DNMs in the ~66.7 Mb of sequenced functional sites (nonsynonymous and splicing). Instead, we identified nine functional p.DNMs, representing a significant enrichment in functional versus neutral DNMs in the NSID cohort ($p = 0.001$). This excess remained significant even when we accounted for the fact that CpG dinucleotides mutate at a faster rate than other sites and are more common in exons than introns ($p = 0.002$; Table 4). Finally, we found that the proportion of

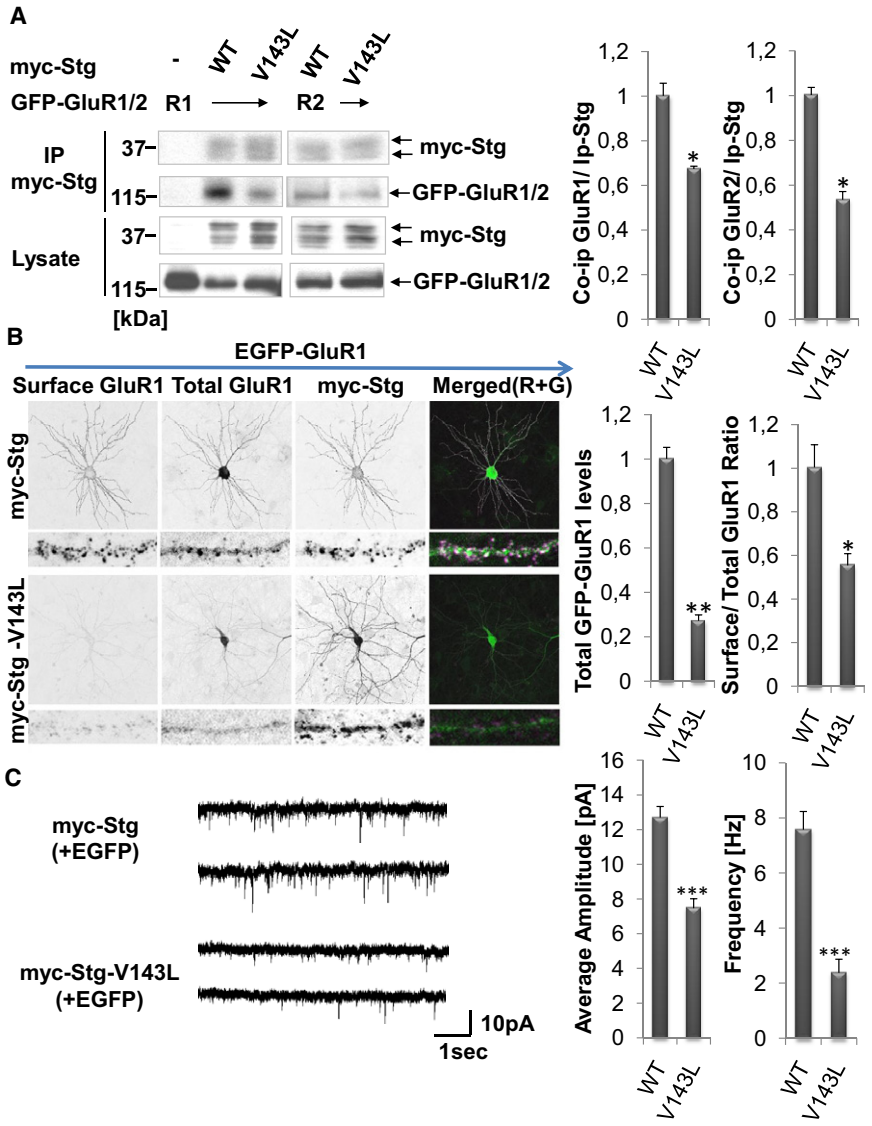

Figure 4. Functional Impact of the p.Val143Leu CACNG2 Mutation

(A) Indicated combinations of expression plasmids (wild-type myc-tagged stargazin [myc-Stg], myc-tagged stargazin-V143L [V143L], GFP-GluR1, GFP-GluR2) were co-transfected in HEK293 cells, and extracted proteins were immunoprecipitated with an anti-myc antibody and then analyzed by immunoblotting with anti-myc or anti-GFP antibodies. The amount of coIP of AMPARs (both GluR1 and GluR2) with Stg was reduced in the Stg-V143L transfected cells. Right: the quantification of the coIP experiments (mean ± SEM, n = 3, *$p < 0.05$, t test).

(B) Hippocampal neurons were transfected with GFP-GluR1 and indicated Stg constructs at DIV19 and stained with an anti-GFP (to detect surface GluR1) in nonpermeabilized conditions at DIV20. Stg-V143L results in reduced surface and total GluR1. Right: quantification of staining results (mean ± SEM, n = 4, **$p < 0.01$, *$p < 0.05$, t test).

(C) Hippocampal neurons were cotransfected with the indicated Stg constructs and GFP at DIV19, and miniature EPSCs were recorded at DIV22/23 from GFP-expressing neurons. Recordings were done in voltage-clamp mode at 65 mV in the presence of an extracellular solution containing 0.5 μM tetrodotoxin (TTX)/100 μM picrotoxin to detect excitatory mEPSC events. Expression of Stg-V143L mutant decreases both mEPSC amplitude and frequency. Right: results quantification (mean ± SEM, n = 4, *$p < 0.05$, t test, ***$p < 0.001$, t test).

functional p.DNMs to neutral ones was increased when compared to all segregating or unique variants ($p < 0.001$; Table 5). We did not include INDEL DNMs in all these comparisons because no neutral INDELs (e.g., affecting nonsplicing intronic sites) were identified.

Discussion

Pathogenicity of the De Novo Truncating Mutations

The truncating DNMs identified in *SYNGAP1* and *STXBP1* are likely pathogenic based on the observations that (1) truncating mutations were not found in these genes in a large series of controls, (2) truncations of the corresponding proteins abolish important functional domains, and (3) haploinsufficiency of these genes affects cognitive processes and/or neurotransmission in mice.[13,24] The splicing DNM identified in *SHANK3* is also likely pathogenic based on its functional impact and the documented involvement of *SHANK3* in related neurodevelopmental diseases. SHANK3 is a PDZ-containing scaffold protein that is localized in the postsynaptic density, where it associates with glutamate receptors and promotes formation of functional synapses.[36–38] The splicing DNM identified here in *SHANK3* is predicted to cause a frameshift upstream of the PDZ domain and Homer and cortactin binding sites (Figure S1), a region where pathogenic *SHANK3* DNMs were previously reported in autism and schizophrenia.[25,26,39]

Pathogenicity of the De Novo Missense and In-Frame Duplication Mutations

Missense DNMs were identified in *KIF1A*, *GRIN1*, *EPB41L1*, and *CACNG2* in the course of the initial NSID cohort screen. Subsequently, sequencing these genes in 50 additional NSID patients identified a second DNM in *GRIN1*, resulting in an in-frame duplication of an amino acid. These DNMs involve well-conserved residues, are predicted to be damaging, and affect protein function in cell culture systems. Although sequencing these genes in larger

Table 4. Base Pairs Sequenced and Point Substitution DNMs Identified

	Initial Count	CpG	Non-CpG	Effective Count
Functional				
NS	64,601,865	1,808,852	62,793,013	80,881,535
Splice	2,144,740	21,447	2,123,293	2,337,767
Total	66,746,605	1,830,300	64,916,306	83,219,302
p.DNMs	9	4	5	9
Neutral				
Syn	26,131,092	731,671	25,399,421	32,716,127
Intronic	80,932,933	809,329	80,123,604	88,216,897
Total	107,064,025	1,541,000	105,523,025	120,933,024
p.DNMs	1	0	1	1
p value	0.001			0.002

The following abbreviations are used: NS, nonsynonymous (missense, nonsense); syn, synonymous; p.DNMs, point substitution DNMs. Nonsynonymous and synonymous sites were estimated at 71.2% and 28.8% of coding sites, respectively. Effective count accounts for increased CpG mutation rate = CpG × 10 + non-CpG sites, where CpG sites were estimated to constitute 2.8% of initial coding sites and 1% of intronic sites.[14] p value, Fisher's exact test.

Table 5. Comparison of p.DNMs to Segregating Variants

	Functional	Neutral	Functional/ Neutral	p Value
p.DNMs	9	1	9	
Unique variants	229	410	0.56	<0.001
All variants	460	1825	0.25	<0.001

Functional denotes nonsynonymus + splice variants. Neutral denotes synonymus + nonsplice intronic sites variants. p value, Fisher's exact test.

cohorts is needed to further ascertain their involvement in NSID, genetic and functional evidence argue in favor of this possibility. Homozygous deletion of *Kif1a* in mice results in insufficient neuronal contact and impaired neurotransmission, leading to perinatal death.[40] Several de novo deletions encompassing *KIF1A* and other genes have been reported in patients with ID and autism, further suggesting that heterozygous *KIF1A* disruption may be involved in NSID.[41] Our functional studies indicate that p.Thr99Met impairs the ability of KIF1A to localize to distal aspects of neurites, consistent with the fact that the Thr^{99} residue lies in the conserved ATP-binding p loop of the motor domain of KIF1A. Interestingly, the heterozygous p.Gln98Leu mutation in KIF1Bβ (MIM 605995), which was reported in a family with autosomal-dominant peripheral neuropathy, affects a residue immediately adjacent to Thr^{99} in the conserved ATP-binding domain ($GQ^{98}T^{99}XXGKT/S$).[42] Although KIF1A and KIF1Bβ share a similar primary structure, their expression patterns and the composition of their cargo are somewhat different, possibly explaining the distinct phenotypes associated with these genes.[30] Nonetheless, even though nerve conduction velocities were normal in our patient, the development of a neuropathy at a later age cannot be ruled out. KIF1A can homodimerize, raising the possibility that deleterious heterozygous mutations at critical sites may act as dominant negatives.[43] Additional work is needed to investigate whether this is the case for p.Thr99Met.

GRIN1 encodes NR1, an essential subunit of the NMDAR that plays a critical role in synaptic plasticity and learning and memory. Homozygous NR1 deletions are embryonic lethal, whereas reduced NR1 expression in mice results in behavioral abnormalities and impaired synaptic plasticity and memory.[44–46] Moreover, de novo deleterious mutations in *GRIN2A* and *GRIN2B*, which encode the two main subunits that associate with GRIN1 to form functional NMDARs, were recently reported in patients with ID.[10] The p.Glu662Lys mutation caused a significant increase in NMDAR-induced Ca^{2+} currents. Excessive Ca^{2+} influx through NMDAR could lead to excitatoxic neuronal cell damage,[47,48] which may, in turn, be responsible for cognitive deficits. On the other hand, the p.Ser560dup almost abolished the activity of the receptor. This may be explained by the significant structural change that this insertion is predicted to cause at the entrance of the channel pore. Collectively, these observations suggest that the *GRIN1* DNMs identified herein may be pathogenic.

The two other missense DNMs reported herein were found in *CACNG2* and *EPB41L1*, which encode AMPAR adaptor proteins that regulate the trafficking and/or activity of the receptor.[18,19,32,33] Transfection studies in HEK293 cells and hippocampal neurons showed that both DNMs caused a significant reduction in the ability of stargazin and 4.1N to bind to AMPAR, resulting in a decrease in the surface expression of GluR1/2 subunits. Abnormal AMPAR trafficking and/or activity has been linked to ID, as outlined below, suggesting a possible mechanism for the potential pathogenicity of these DNMs.

Disruption of AMPAR Signaling and/or Trafficking in NSID

The majority of the DNMs reported herein affect genes that are involved directly or indirectly in AMPAR trafficking. Indeed, EPB41L1, CACNG2, and SYNGAP1 have all been shown to regulate AMPAR trafficking.[19,33,49] Furthermore, emerging evidence also suggests that KIF1A, SHANK3, and GRIN1 may also play a role in regulating AMPAR trafficking. KIF1A interacts with AMPARs via its liprin-alpha domain, and therefore could potentially act as a neuronal AMPAR transporter.[31] SHANK3 has been reported to directly interact with GluR1 and to influence the recruitment of functional AMPARs to dendritic spines.[37,38] As for GRIN1, a recent report showed that phosphorylation of NR1 at certain residues reduces synaptic AMPAR levels in vivo.[50] Moreover, NMDAR activity can influence pathways involved in the regulation of AMPAR trafficking. Regulation of AMPAR trafficking is critical for synaptic plasticity and learning and memory,

and dysfunction of this process has the potential of causing cognitive disorders.[51] For instance, mutations in *GRIA3*, which encodes for an AMPAR subunit, and in several genes known to affect AMPAR trafficking (such as *PAK3* [MIM 300142], *OPHN1* [MIM 300127], *FMR1*, and *DLG3* [MIM 300189]) have been previously shown to cause forms of ID.[1,12,52–55]

Contribution of DNMs in Synaptic Genes to NSID

By focusing our resequencing effort on candidate GRC genes, we identified DNMs in ~11% of the NSID cases. The fact that 10 out of the 11 DNMs were functional and likely pathogenic supports the role of DNMs in NSID and highlights the importance of the glutamatergic pathways in this disease. This is in agreement with a recent exome sequencing of ten individuals with ID and identification of nine DNMs, two of which were truncations in known ID synaptic genes, *RAB39B* (MIM 300774) and *SYNGAP1*.[56] Finally, recent sequencing of candidate synaptic genes in autism spectrum disorders and schizophrenia also reported an excess of functional DNMs in these diseases.[14] This observation further supports the notion that ID, autism spectrum disorders, and schizophrenia may share a common synaptic component.

Supplemental Data

Supplemental Data include five figures and five tables and can be found with this article online at http://www.cell.com/AJHG/.

Acknowledgments

Supported by grants from the Canadian Institute of Health Research (to J.C.L., G.A.R., and J.L.M.), Réseau de Médecine Génétique Appliquée (FRSQ; to J.L.M.), Genome Canada, and Genome Quebec, with cofunding by Université de Montréal (to P.D. and G.A.R.). J.L.M. holds a FRSQ National Scientist Award. The S2D group includes Yan Yang, Anne Noreau, Annie Raymond, Annie Levert, Pascale Thibodeau, Mélanie Coté, Frédéric Kuku, Sandra Laurent, Philippe Jolivet, Joannie Duguay, Karine Lachapelle, and Isabelle Bachand. We thank the patients and their parents for participating in this study. We thank Philip Awadalla for useful discussions. We are thankful to the members of McGill University and Génome Québec Innovation Centre Sequencing (Pierre Lepage, Sébastien Brunet, and Hao Fan Yam) and Bioinformatic (Louis Létourneau and Louis Dumond Joseph) groups.

Received: December 16, 2010
Revised: January 27, 2011
Accepted: February 1, 2011
Published online: March 3, 2011

Web Resources

The URLs for data presented herein are as follows:

dbSNP, http://www.ncbi.nlm.nih.gov/projects/SNP/
Genes to Cognition, http://www.g2conline.org/
McGill University and Génome Québec Innovation Centre, http://gqinnovationcenter.com/index.aspx
Online Mendelian Inheritance in Man (OMIM), http://www.ncbi.nlm.nih.gov/Omim/
Panther, http://www.pantherdb.org
Polyphen, http://genetics.bwh.harvard.edu/pph/
RCSB Protein Data Bank, http://www.rcsb.org
SIFT, http://sift.jcvi.org
SWISS-MODEL Workspace, http://swissmodel.expasy.org
UCSC Genome Browser, http://www.genome.ucsc.edu/
Uniprot protein sequence and functional information browser, http://www.uniprot.org/

References

1. Kaufman, L., Ayub, M., and Vincent, J.B. (2010). The genetic basis of non-syndromic intellectual disability: A review. J. Neurodev. Disord. *2*, 182–209.
2. Ropers, H.H. (2010). Genetics of early onset cognitive impairment. Annu. Rev. Genomics Hum. Genet. *11*, 161–187.
3. Laumonnier, F., Cuthbert, P.C., and Grant, S.G. (2007). The role of neuronal complexes in human X-linked brain diseases. Am. J. Hum. Genet. *80*, 205–220.
4. Pocklington, A.J., Cumiskey, M., Armstrong, J.D., and Grant, S.G. (2006). The proteomes of neurotransmitter receptor complexes form modular networks with distributed functionality underlying plasticity and behaviour. Mol. Syst. Biol. *2*, 23.
5. Collins, M.O., Husi, H., Yu, L., Brandon, J.M., Anderson, C.N., Blackstock, W.P., Choudhary, J.S., and Grant, S.G. (2006). Molecular characterization and comparison of the components and multiprotein complexes in the postsynaptic proteome. J. Neurochem. *97* (*Suppl 1*), 16–23.
6. Kessels, H.W., and Malinow, R. (2009). Synaptic AMPA receptor plasticity and behavior. Neuron *61*, 340–350.
7. Lerma, J. (2006). Kainate receptor physiology. Curr. Opin. Pharmacol. *6*, 89–97.
8. Rao, V.R., and Finkbeiner, S. (2007). NMDA and AMPA receptors: Old channels, new tricks. Trends Neurosci. *30*, 284–291.
9. Simonyi, A., Schachtman, T.R., and Christoffersen, G.R. (2005). The role of metabotropic glutamate receptor 5 in learning and memory processes. Drug News Perspect. *18*, 353–361.
10. Endele, S., Rosenberger, G., Geider, K., Popp, B., Tamer, C., Stefanova, I., Milh, M., Kortüm, F., Fritsch, A., Pientka, F.K., et al. (2010). Mutations in GRIN2A and GRIN2B encoding regulatory subunits of NMDA receptors cause variable neurodevelopmental phenotypes. Nat. Genet. *42*, 1021–1026.
11. Motazacker, M.M., Rost, B.R., Hucho, T., Garshasbi, M., Kahrizi, K., Ullmann, R., Abedini, S.S., Nieh, S.E., Amini, S.H., Goswami, C., et al. (2007). A defect in the ionotropic glutamate receptor 6 gene (GRIK2) is associated with autosomal recessive mental retardation. Am. J. Hum. Genet. *81*, 792–798.
12. Wu, Y., Arai, A.C., Rumbaugh, G., Srivastava, A.K., Turner, G., Hayashi, T., Suzuki, E., Jiang, Y., Zhang, L., Rodriguez, J., et al. (2007). Mutations in ionotropic AMPA receptor 3 alter channel properties and are associated with moderate cognitive impairment in humans. Proc. Natl. Acad. Sci. USA *104*, 18163–18168.
13. Hamdan, F.F., Gauthier, J., Spiegelman, D., Noreau, A., Yang, Y., Pellerin, S., Dobrzeniecka, S., Côté, M., Perreau-Linck, E., Carmant, L., et al; Synapse to Disease Group. (2009). Mutations in SYNGAP1 in autosomal nonsyndromic mental retardation. N. Engl. J. Med. *360*, 599–605.

14. Awadalla, P., Gauthier, J., Myers, R.A., Casals, F., Hamdan, F.F., Griffing, A.R., Côté, M., Henrion, E., Spiegelman, D., Tarabeux, J., et al. (2010). Direct measure of the de novo mutation rate in autism and schizophrenia cohorts. Am. J. Hum. Genet. *87*, 316–324.
15. Lee, J.R., Shin, H., Choi, J., Ko, J., Kim, S., Lee, H.W., Kim, K., Rho, S.H., Lee, J.H., Song, H.E., et al. (2004). An intramolecular interaction between the FHA domain and a coiled coil negatively regulates the kinesin motor KIF1A. EMBO J. *23*, 1506–1515.
16. Jin, L., Miyazaki, M., Mizuno, S., Takigawa, M., Hirose, T., Nishimura, K., Toida, T., Williams, K., Kashiwagi, K., and Igarashi, K. (2008). The pore region of N-methyl-D-aspartate receptors differentially influences stimulation and block by spermine. J. Pharmacol. Exp. Ther. *327*, 68–77.
17. Mi, R., Sia, G.M., Rosen, K., Tang, X., Moghekar, A., Black, J.L., McEnery, M., Huganir, R.L., and O'Brien, R.J. (2004). AMPA receptor-dependent clustering of synaptic NMDA receptors is mediated by Stargazin and NR2A/B in spinal neurons and hippocampal interneurons. Neuron *44*, 335–349.
18. Lin, D.T., Makino, Y., Sharma, K., Hayashi, T., Neve, R., Takamiya, K., and Huganir, R.L. (2009). Regulation of AMPA receptor extrasynaptic insertion by 4.1N, phosphorylation and palmitoylation. Nat. Neurosci. *12*, 879–887.
19. Shen, L., Liang, F., Walensky, L.D., and Huganir, R.L. (2000). Regulation of AMPA receptor GluR1 subunit surface expression by a 4. 1N-linked actin cytoskeletal association. J. Neurosci. *20*, 7932–7940.
20. Lee, J.R., Shin, H., Ko, J., Choi, J., Lee, H., and Kim, E. (2003). Characterization of the movement of the kinesin motor KIF1A in living cultured neurons. J. Biol. Chem. *278*, 2624–2629.
21. Arnold, K., Bordoli, L., Kopp, J., and Schwede, T. (2006). The SWISS-MODEL workspace: A web-based environment for protein structure homology modelling. Bioinformatics *22*, 195–201.
22. Bordoli, L., Kiefer, F., Arnold, K., Benkert, P., Battey, J., and Schwede, T. (2009). Protein structure homology modeling using SWISS-MODEL workspace. Nat. Protoc. *4*, 1–13.
23. Sobolevsky, A.I., Rosconi, M.P., and Gouaux, E. (2009). X-ray structure, symmetry and mechanism of an AMPA-subtype glutamate receptor. Nature *462*, 745–756.
24. Hamdan, F.F., Piton, A., Gauthier, J., Lortie, A., Dubeau, F., Dobrzeniecka, S., Spiegelman, D., Noreau, A., Pellerin, S., Côté, M., et al. (2009). De novo STXBP1 mutations in mental retardation and nonsyndromic epilepsy. Ann. Neurol. *65*, 748–753.
25. Gauthier, J., Champagne, N., Lafrenière, R.G., Xiong, L., Spiegelman, D., Brustein, E., Lapointe, M., Peng, H., Côté, M., Noreau, A., et al; S2D Team. (2010). De novo mutations in the gene encoding the synaptic scaffolding protein SHANK3 in patients ascertained for schizophrenia. Proc. Natl. Acad. Sci. USA *107*, 7863–7868.
26. Gauthier, J., Spiegelman, D., Piton, A., Lafrenière, R.G., Laurent, S., St-Onge, J., Lapointe, L., Hamdan, F.F., Cossette, P., Mottron, L., et al. (2009). Novel de novo SHANK3 mutation in autistic patients. Am. J. Med. Genet. B. Neuropsychiatr. Genet. *150B*, 421–424.
27. Ng, P.C., and Henikoff, S. (2003). SIFT: Predicting amino acid changes that affect protein function. Nucleic Acids Res. *31*, 3812–3814.
28. Sunyaev, S., Ramensky, V., Koch, I., Lathe, W., 3rd, Kondrashov, A.S., and Bork, P. (2001). Prediction of deleterious human alleles. Hum. Mol. Genet. *10*, 591–597.
29. Thomas, P.D., Kejariwal, A., Guo, N., Mi, H., Campbell, M.J., Muruganujan, A., and Lazareva-Ulitsky, B. (2006). Applications for protein sequence-function evolution data: mRNA/protein expression analysis and coding SNP scoring tools. Nucleic Acids Res. *34* (Web Server issue), W645-50.
30. Hirokawa, N., Noda, Y., Tanaka, Y., and Niwa, S. (2009). Kinesin superfamily motor proteins and intracellular transport. Nat. Rev. Mol. Cell Biol. *10*, 682–696.
31. Shin, H., Wyszynski, M., Huh, K.H., Valtschanoff, J.G., Lee, J.R., Ko, J., Streuli, M., Weinberg, R.J., Sheng, M., and Kim, E. (2003). Association of the kinesin motor KIF1A with the multimodular protein liprin-alpha. J. Biol. Chem. *278*, 11393–11401.
32. Tomita, S., Adesnik, H., Sekiguchi, M., Zhang, W., Wada, K., Howe, J.R., Nicoll, R.A., and Bredt, D.S. (2005). Stargazin modulates AMPA receptor gating and trafficking by distinct domains. Nature *435*, 1052–1058.
33. Chen, L., Chetkovich, D.M., Petralia, R.S., Sweeney, N.T., Kawasaki, Y., Wenthold, R.J., Bredt, D.S., and Nicoll, R.A. (2000). Stargazin regulates synaptic targeting of AMPA receptors by two distinct mechanisms. Nature *408*, 936–943.
34. Roach, J.C., Glusman, G., Smit, A.F., Huff, C.D., Hubley, R., Shannon, P.T., Rowen, L., Pant, K.P., Goodman, N., Bamshad, M., et al. (2010). Analysis of genetic inheritance in a family quartet by whole-genome sequencing. Science *328*, 636–639.
35. Durbin, R.M., Abecasis, G.R., Altshuler, D.L., Auton, A., Brooks, L.D., Durbin, R.M., Gibbs, R.A., Hurles, M.E., and McVean, G.A.; 1000 Genomes Project Consortium. (2010). A map of human genome variation from population-scale sequencing. Nature *467*, 1061–1073.
36. Baron, M.K., Boeckers, T.M., Vaida, B., Faham, S., Gingery, M., Sawaya, M.R., Salyer, D., Gundelfinger, E.D., and Bowie, J.U. (2006). An architectural framework that may lie at the core of the postsynaptic density. Science *311*, 531–535.
37. Uchino, S., Wada, H., Honda, S., Nakamura, Y., Ondo, Y., Uchiyama, T., Tsutsumi, M., Suzuki, E., Hirasawa, T., and Kohsaka, S. (2006). Direct interaction of post-synaptic density-95/Dlg/ZO-1 domain-containing synaptic molecule Shank3 with GluR1 alpha-amino-3-hydroxy-5-methyl-4-isoxazole propionic acid receptor. J. Neurochem. *97*, 1203–1214.
38. Roussignol, G., Ango, F., Romorini, S., Tu, J.C., Sala, C., Worley, P.F., Bockaert, J., and Fagni, L. (2005). Shank expression is sufficient to induce functional dendritic spine synapses in aspiny neurons. J. Neurosci. *25*, 3560–3570.
39. Durand, C.M., Betancur, C., Boeckers, T.M., Bockmann, J., Chaste, P., Fauchereau, F., Nygren, G., Rastam, M., Gillberg, I.C., Anckarsäter, H., et al. (2007). Mutations in the gene encoding the synaptic scaffolding protein SHANK3 are associated with autism spectrum disorders. Nat. Genet. *39*, 25–27.
40. Yonekawa, Y., Harada, A., Okada, Y., Funakoshi, T., Kanai, Y., Takei, Y., Terada, S., Noda, T., and Hirokawa, N. (1998). Defect in synaptic vesicle precursor transport and neuronal cell death in KIF1A motor protein-deficient mice. J. Cell Biol. *141*, 431–441.
41. Galasso, C., Lo-Castro, A., Lalli, C., Nardone, A.M., Gullotta, F., and Curatolo, P. (2008). Deletion 2q37: An identifiable clinical syndrome with mental retardation and autism. J. Child Neurol. *23*, 802–806.
42. Zhao, C., Takita, J., Tanaka, Y., Setou, M., Nakagawa, T., Takeda, S., Yang, H.W., Terada, S., Nakata, T., Takei, Y., et al.

(2001). Charcot-Marie-Tooth disease type 2A caused by mutation in a microtubule motor KIF1Bbeta. Cell *105*, 587–597.
43. Hammond, J.W., Cai, D., Blasius, T.L., Li, Z., Jiang, Y., Jih, G.T., Meyhofer, E., and Verhey, K.J. (2009). Mammalian Kinesin-3 motors are dimeric in vivo and move by processive motility upon release of autoinhibition. PLoS Biol. *7*, e72.
44. Cui, Z., Wang, H., Tan, Y., Zaia, K.A., Zhang, S., and Tsien, J.Z. (2004). Inducible and reversible NR1 knockout reveals crucial role of the NMDA receptor in preserving remote memories in the brain. Neuron *41*, 781–793.
45. Forrest, D., Yuzaki, M., Soares, H.D., Ng, L., Luk, D.C., Sheng, M., Stewart, C.L., Morgan, J.I., Connor, J.A., and Curran, T. (1994). Targeted disruption of NMDA receptor 1 gene abolishes NMDA response and results in neonatal death. Neuron *13*, 325–338.
46. Mohn, A.R., Gainetdinov, R.R., Caron, M.G., and Koller, B.H. (1999). Mice with reduced NMDA receptor expression display behaviors related to schizophrenia. Cell *98*, 427–436.
47. MacDonald, J.F., Xiong, Z.G., and Jackson, M.F. (2006). Paradox of Ca2+ signaling, cell death and stroke. Trends Neurosci. *29*, 75–81.
48. Nakamura, T., and Lipton, S.A. (2007). S-Nitrosylation and uncompetitive/fast off-rate (UFO) drug therapy in neurodegenerative disorders of protein misfolding. Cell Death Differ. *14*, 1305–1314.
49. Rumbaugh, G., Adams, J.P., Kim, J.H., and Huganir, R.L. (2006). SynGAP regulates synaptic strength and mitogen-activated protein kinases in cultured neurons. Proc. Natl. Acad. Sci. USA *103*, 4344–4351.
50. Li, B., Devidze, N., Barengolts, D., Prostak, N., Sphicas, E., Apicella, A.J., Malinow, R., and Emamian, E.S. (2009). NMDA receptor phosphorylation at a site affected in schizophrenia controls synaptic and behavioral plasticity. J. Neurosci. *29*, 11965–11972.
51. Shepherd, J.D., and Huganir, R.L. (2007). The cell biology of synaptic plasticity: AMPA receptor trafficking. Annu. Rev. Cell Dev. Biol. *23*, 613–643.
52. Boda, B., Alberi, S., Nikonenko, I., Node-Langlois, R., Jourdain, P., Moosmayer, M., Parisi-Jourdain, L., and Muller, D. (2004). The mental retardation protein PAK3 contributes to synapse formation and plasticity in hippocampus. J. Neurosci. *24*, 10816–10825.
53. Elias, G.M., Elias, L.A., Apostolides, P.F., Kriegstein, A.R., and Nicoll, R.A. (2008). Differential trafficking of AMPA and NMDA receptors by SAP102 and PSD-95 underlies synapse development. Proc. Natl. Acad. Sci. USA *105*, 20953–20958.
54. Hu, H., Qin, Y., Bochorishvili, G., Zhu, Y., van Aelst, L., and Zhu, J.J. (2008). Ras signaling mechanisms underlying impaired GluR1-dependent plasticity associated with fragile X syndrome. J. Neurosci. *28*, 7847–7862.
55. Nadif Kasri, N., Nakano-Kobayashi, A., Malinow, R., Li, B., and Van Aelst, L. (2009). The Rho-linked mental retardation protein oligophrenin-1 controls synapse maturation and plasticity by stabilizing AMPA receptors. Genes Dev. *23*, 1289–1302.
56. Vissers, L.E., de Ligt, J., Gilissen, C., Janssen, I., Steehouwer, M., de Vries, P., van Lier, B., Arts, P., Wieskamp, N., del Rosario, M., et al. (2010). A de novo paradigm for mental retardation. Nat. Genet. *42*, 1109–1112.